

# Analysis of thermomechanical interactions and properties of ceramic breeder blankets

Alice Ying \*, Mohamed Abdou

*Mechanical and Aerospace Engineering Department, UCLA, Los Angeles CA 90095-1597, USA*

---

## Abstract

Analysis of the thermomechanical interactions of fusion blanket materials and physical elements, particularly those involving particle bed design concepts, have been performed. The results show that the stress caused by the high thermal expansion of the blanket particle bed material is not excessive enough to be of concern for the structural material. However, its magnitude could lead to ceramic particle breakage if the bed behaves like a solid material. Furthermore, the calculations show that the clad deflection caused by this stress could lead to a possible separation between the bed and clad, which would add an unfavorable thermal resistance to the region and increase local temperature. A comparison between the estimated stress extrapolated from the experimental data and the analytical results shows that the thermomechanical performance of the pebble bed approaches that of solid materials. © 1998 Elsevier Science S.A. All rights reserved.

---

## 1. Introduction

High volumetric heat generation rates and low thermal conductivity cause large temperature gradients in the breeder elements. These temperature differences produce expansion of materials and if no restraints, both internal and external, are placed on materials, they expand in a stress-free manner. However, interconnecting components produce external restraints on expansion and thermal stresses result in blanket elements. Thus, potential failure due to thermal stresses places constraints on the blanket performance. One might argue that ceramic breeders have no structural role; however, their thermomechanical behavior is important from a cracking-resistance perspective.

Breeder cracking is undesirable since it alters heat transfer characteristics and may cause tritium purge channel plugging due to transport and relocation of breeder fragments by the purge gas. Consequently, it is very important to be able to accurately predict the state of the stress in the blanket element to insure that a failure does not occur.

Substantial experimental and modeling efforts have been carried out to characterize the most important properties that directly affect the blanket thermal performances. These properties include effective thermal conductivity, pebble bed wall conductance, and interface conductance between sintered Be and stainless steel cladding. Good agreement has been obtained for the effective thermal conductivity of single-size pebble beds. The most uncertainty exists in the experi-

---

\* Corresponding author.

mental database and model prediction capability of the pebble bed wall conductance [1] which is generally influenced by less quantifiable parameters such as packing geometry, contact force and porosity distributions. It is further affected by the bed/clad interaction. For example, low value of interface conductance obtained experimentally might be the result of the bed/clad separation due to thin clad bowing during operation [2]. On the other hand, it is known that the induced thermal stresses alter particle contact characteristics and increase the amount of contact area which could lead to enhancement of the packed bed effective thermal conductivity. With this in mind, this paper focuses on the analysis of the thermomechanical interaction of fusion blanket elements particularly those involving particle bed design concepts. Experimental data related to the thermomechanical interaction are first examined followed by the thermomechanical analysis of the blanket unit cell. The stress exerted on the cladding wall due to bed thermal expansion is calculated utilizing experimental particle bed effective modulus data. The force transmitted at the contact point is discussed and compared with available experimental data.

## 2. Analysis of experimental data related to thermomechanical interactions

In this section, previous experimental studies on the thermomechanical interactions related to the ceramic breeder blankets are discussed. The heat transfer data from Dalle Donne et al. [3] has shown that for the same average bed temperature, a larger temperature gradient across the blanket provides a higher effective thermal conductivity. These experiments were carried out for aluminum particle beds (to simulate beryllium packed beds) at different temperature gradients ( $\Delta T$ ). The heat transfer enhancement is caused by the difference in the thermal expansion coefficient of the aluminum and cladding material. Aluminum has a higher thermal expansion coefficient and consequently the aluminum particles are pressed together more strongly and the contact area

between the pebbles increases. To reflect this phenomenon the data of the bed effective thermal conductivity ( $k$ ) has been correlated as [3]

$$k = C_0 [T(^{\circ}\text{C})]^{0.1721} [\Delta T(^{\circ}\text{C})]^{0.1173} \quad (1)$$

where  $C_0$  is a constant. The increase in the effective thermal conductivity caused by the temperature difference can be related to the increase in the contact area of the particulate. In Fig. 1, the calculated average increase in the fractional contact area (based on the analysis of Wakao et al. [4]) and the corresponding normal constrained displacement at the contact point causing this contact area are plotted as a function of temperature difference. These calculations show that a slight increase in the contact area of 0.024% at the particle contact point can lead to an increase of the aluminum bed effective thermal conductivity by a factor of 2.

According to Hertz's theory [5], it is conceivable to estimate the normal force ( $P$ ) exerted on the contact point to respond to this normal constrained displacement:

$$P = M \left( \frac{3\delta}{R} \right)^{1.5} \quad (2)$$

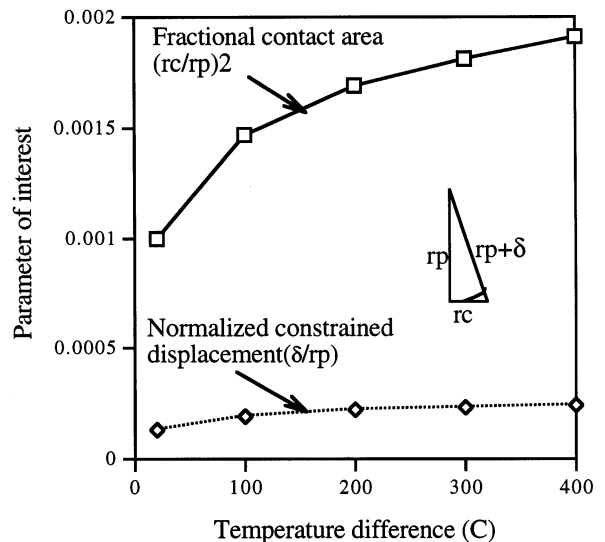


Fig. 1. Fractional contact area and normalized constrained displacement as a function of temperature difference.

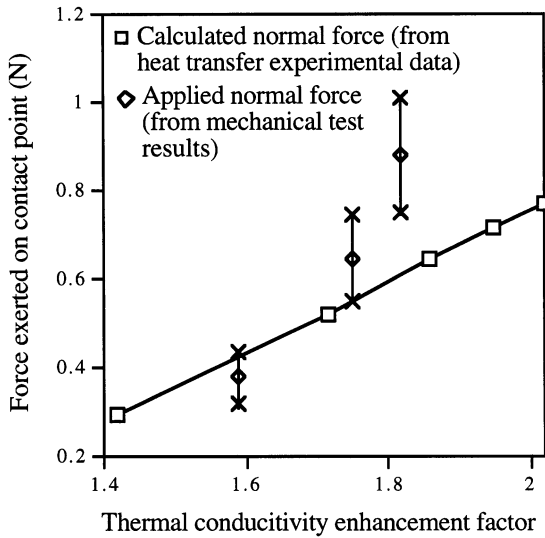


Fig. 2. Comparison of mechanically applied forces and thermally induced forces for achieving the same magnitudes of thermal conductivity enhancement.

where  $\delta$  and  $R$  are the normal displacement and particle radius, respectively, and  $M$  is given in terms of the shear modulus  $G$  and Poisson's ratio  $\nu$  of the material of the spheres by:

$$M = \frac{8}{9\sqrt{3}} \frac{GR^2}{(1-\nu)} \tag{3}$$

The calculated  $P$  is plotted as a function of thermal conductivity enhancement in Fig. 2 and compared with the experimental data of Tehranian et al. [6] in which the experiments were carried out to study the effect of the applied mechanical load on heat transfer enhancement. The comparison shows a reasonable agreement between the applied mechanical loads and the thermally induced stresses that obtain the same magnitude of bed heat transfer enhancement. Since this normal force originates from the constrained bed thermal expansion which is caused by the temperature rise of the bed, the relationship between the macro-scale stress exerted on the clad and the aforementioned force is addressed in the later section.

### 3. Thermomechanical interaction analysis model

In an attempt to explain how the heat transfer and contact area increase and to estimate the stress of the state at the containment wall as a result of the differential thermal expansion, a thermomechanical model is developed for a typical blanket unit cell involving a packed bed regime with its associated containment clad. The model is derived from Euler-Bernoulli's equation, which was also used in a previous thermomechanical analysis [7]. When compared to the previous model, the present analysis has the following distinguished features: (1) it utilizes an experimental value of the packed bed effective modulus for stress [8] calculations; (2) since there is, as of yet, no adequate model for describing particle bed macroscopic mechanical behavior, analyses are performed for both solid- and fluid-like behaviors, and (3) the model allows no stress to exert on the containment wall where the bed expands less than the wall deformation. Furthermore, the model decouples the microscopic effect from the macro-scale behavior considering that no adequate microphysical properties and constitutive equations are available for describing the complex phenomena involved at the microscopic level. The interparticle mechanical quantities at microscopic level are analyzed once the stress is calculated.

For the unit cell as shown in Fig. 3, the total unrestrained deformation of the particle bed in the  $y$  direction due to a uniform temperature rise  $\Delta T$  given by:

$$\Delta y = \alpha_p \Delta T W \tag{4}$$

If the particle bed is assumed to behave like a solid continuous material, then the bed-clad contact stress ( $\sigma$ ) would be equal to

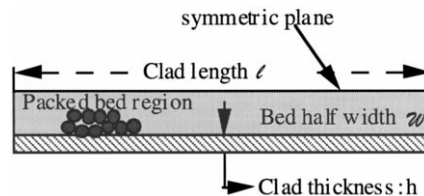


Fig. 3. Schematic view of thermomechanical interaction analytical model (clamped boundaries at both ends).

$$\sigma = E_p \frac{\Delta y - \delta x}{W} \quad (5)$$

where  $E_p$  is the particle bed effective Young's modulus,  $W$  is the bed half-width, and  $\delta(x)$  is the amount of clad deflection. If  $\Delta y < \delta(x)$ , this means that no contact is established at the structural/bed interface and accordingly the aforementioned stress is set to 0. By assuming that the deflection of the structural clad is governed by the Euler-Bernoulli equations, which states:

$$E_s I \frac{d^4 \delta(x)}{dx^4} = \sigma D \quad (6)$$

where  $I$  is given as

$$I = \frac{h^3 D}{12} \quad (7)$$

and  $E_s$  is the Young's modulus of the containing structural wall, and  $D$  and  $h$  are the bed height and containment clad thickness. Substituting Eqs. (4) and (5) into Eq. (6) we have

$$\frac{d^4 \delta(x)}{dx^4} = \frac{E_p D}{E_s I} \alpha_p \Delta T W - \frac{E_p D}{E_s I W} \delta(x) \quad \text{if}$$

$$\delta(x) \leq \alpha_p \Delta T W \quad (8)$$

and

$$\frac{d^4 \delta(x)}{dx^4} = 0 \quad \text{if} \quad \delta(x) > \alpha_p \Delta T W \quad (9)$$

with the boundary conditions of

$$\delta\left(-\frac{l}{2}\right) = \delta\left(\frac{l}{2}\right) = 0 \quad (10)$$

$$\delta(x_0^-) = \delta(x_0^+) = \alpha_p \Delta T W \quad (11)$$

and

$$\delta'\left(-\frac{l}{2}\right) = \delta'\left(\frac{l}{2}\right) = 0 \quad (12)$$

$$\delta'(x_0^-) = \delta'(x_0^+) \quad (13)$$

here  $x_0$  is the location where the amount of clad deflection is equal to that of the bed thermal expansion and  $l$  is the bed or clad length.

In the case where the particle bed behaves like the fluid, the stress exerted on the structural clad due to the particle bed thermal expansion will be

equal to a constant. Hence, the Euler–Bernoulli's equation becomes

$$E_s I \frac{d^4 \delta^f(x)}{dx^4} = \sigma^f D \quad (14)$$

with the boundary conditions of

$$\delta^f\left(-\frac{l}{2}\right) = \delta^f\left(\frac{l}{2}\right) = 0$$

$$\delta^f\left(-\frac{l}{2}\right) = \delta^f\left(\frac{l}{2}\right) = 0. \quad (15)$$

The stress can further be related to the strain through Hooke's law

$$\frac{\Delta V}{V} = 2\left(\alpha^p \Delta T - \frac{\sigma^f}{E_p}\right) \quad (16)$$

where  $\Delta V = \Delta A D$  for a 2-D deflection and is calculated as

$$\Delta A = \int_{-1/2}^{1/2} \delta^f(x) dx \quad (17)$$

#### 4. Results

The calculated clad deflection and stress exerted on the cladding wall based on different models of bed behavior are plotted in Figs. 4 and 5 for the ceramic packed bed, respectively, as a function of normalized clad position. In spite of the fact that the experimental data of the packed bed thermal expansion obtained presently at UCLA reveals its dependence on the state of the local stress, the data is not yet comprehensive. Consequently, these calculations are performed using the thermal expansion coefficient data for solid material. The calculations show that the stress caused by the difference in the thermal expansions of the ceramic pebbles and the containment clad could be as high as 4.2 MPa at the corners and drop to zero where the clad deflects more than the bed expands as calculated by the solid model. According to the mechanical test results for  $\text{Li}_2\text{ZrO}_3$  particles (as fabricated), they begin to break at the stress level of about 2.6 MPa [8], this implies that a fraction of particles would be broken during operation according to the solid model calculations. This consequence is also affected by the bed

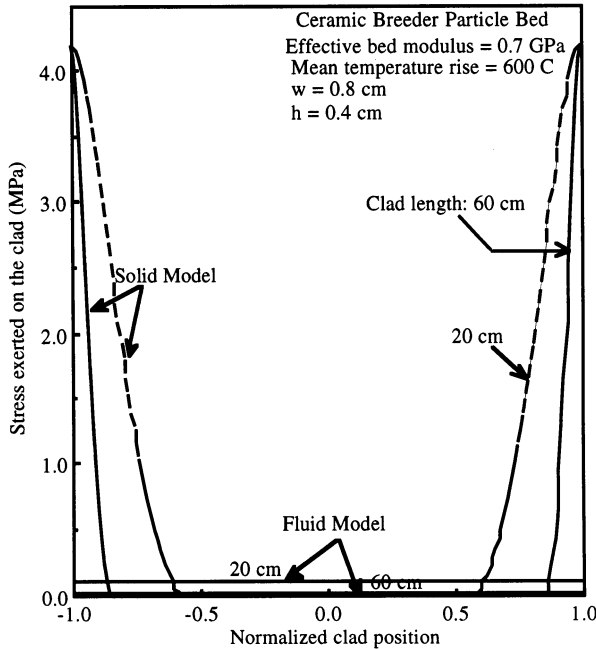


Fig. 4. Calculated ceramic breeder bed clad stress vs normalized clad position using different models.

length, the shorter the bed the larger will be the portion of the containment clad that would exert the stress. The clad deflects more if the bed's behavior approaches that of a fluid. The largest deflection of 175 μm takes place at the center of the clad and is independent of the clad length. The stress on the clad is significantly low based on the fluid model and is about 0.1 MPa for a clad length of 20 cm. The stress is even lower for a longer bed.

Because the effective modulus of the aluminum packed bed is higher than that of the ceramic pebble bed, both the stress and deformation of the wall resulting from the aluminum packed bed thermal expansion are much higher as shown in Figs. 6 and 7, respectively. Again, the magnitude of the stress is much lower with the fluid model assumption. To resolve which model provides a closer solution to the experimental data, the stress which would give an average contact force of  $P$  equal to 0.7697 N, corresponding to an average bed temperature rise of 400°C as presented in the previous section, is estimated using [9]:

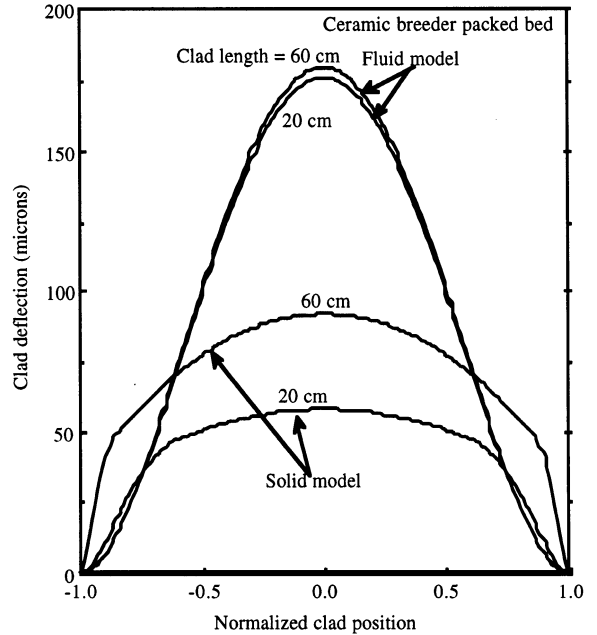


Fig. 5. Calculated ceramic breeder bed clad deflection vs normalized clad position using different models.

$$\sigma = \frac{P(1 - \phi)n}{4\pi R^2} \tag{18}$$

where  $\phi$  is the porosity of the packed bed (= 0.375),  $n$  the average number of contacts per

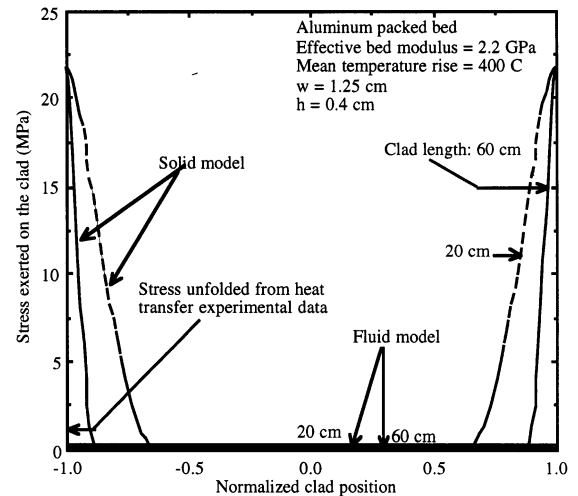


Fig. 6. Calculated aluminum bed clad stress vs normalized clad position using different models.

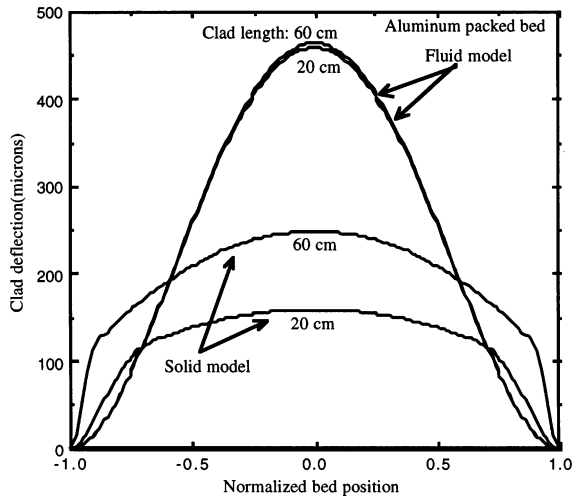


Fig. 7. Calculated aluminum bed clad deflection vs normalized clad position using different models.

particle ( $= 8$ ) and  $R$  particle radius ( $= 1$  mm). The calculated result of 1.24 MPa as shown in Fig. 6 is close to the average value from the solid model and is much higher than the result computed from the fluid model. Although the comparison appears promising for the solid model, one has to realize that the mechanical characteristics at the microscopic level, such as contact points, is much more complicated. It is known that the displacement of a contact point relative to the center of its sphere includes not only the normal displacement but tangential displacement which consists of two terms describing translational displacement between particle centers and rotational. For a dense system where the rotational displacement can be neglected, the force exerted by the sphere at a contact would then have parallel components other than normal components considered in the calculations. The analysis is further complicated by the fact that the packed bed effective modulus is expected to increase as the average bed temperature increases. Thus, in order to accurately predict bed thermomechanical performance, the effective macromechanics parameter, such as the bed effective modulus, and the micromechanics parameter, such as inter-particle friction coefficient, are needed.

## 5. Conclusions

The thermomechanical analysis has shown that the stress resulting from the high thermal expansion of the blanket particle bed material is not excessive enough to be of a concern for the structural material. However, its magnitude could lead to ceramic particle breakage if the bed behaves like the solid material. Furthermore, the calculations show that the clad deflection caused by this stress could lead to a possible bed/clad separation which would add an undesirable thermal resistance to the region and increase local temperature. The calculation shows that the stress exerted on the clad is much smaller if a fluid model is assumed for the bed behavior. The comparison between the estimated stress extrapolated from the experimental data and the analytical results shows that the thermomechanical performance of the pebble bed approaches that of solid material. However, in order to accurately predict bed performance and to understand how the induced/external mechanical force is transmitted through the particle contact points and alters the contact characteristics, it is necessary to better quantify bed behavior and particle bed mechanical properties. More experimental work is needed to determine macro thermomechanical effective properties and micromechanics parameters to better understand the bed thermomechanical interaction. These parameters include the intra-particle friction coefficient, skin friction and contact stiffness under various levels of constraints.

## Acknowledgements

This work was performed under US Department of Energy Contract DE-F603 86ER52123.

## References

- [1] M.C. Billone, Update of beryllium properties and performance, Intra-laboratory Memo, ANL, November, 1995.

- [2] F.F. Sherman, Modeling and experimental results of the UCLA high temperature cyclic experiments, MS Thesis, UCLA, 1995.
- [3] M. Dalle Donne, A. Goraieb, G. Sordon, Measurements of the effective thermal conductivity of a bed of Li<sub>4</sub>SiO<sub>4</sub> pebbles of 0.35–0.6 mm diameter and of a mixed bed of Li<sub>4</sub>SiO<sub>4</sub> and aluminum pebbles, *J. Nucl. Mater.* 191 (194) (1992) 149–152.
- [4] N. Wakao, K. Kato, Effective thermal conductivity of packed beds, *J. Chem. Eng. Jpn* 2 (1) (1969) 24.
- [5] J. Duffy, R.D. Mindlin, Stress–strain relations and vibrations of a granular medium, *J. Appl. Mech.*, December (1957) 585–593.
- [6] F. Tehraniam, M.A. Abdou, M.S. Tillack, Effect of external pressure on particle bed effective thermal conductivity, *J. Nucl. Mater* 885 (1994) 212–215.
- [7] F. Tehranian, R. Hejal, Thermo-mechanical interactions of particle bed/structural wall in a layered configuration, part I, *Fusion Eng. Des.* 27 (1995) 283–289.
- [8] A. Ying, L. Zi, M.A. Abdou, Mechanical behavior and design database of packed beds for blanket designs, *Fusion Eng. Des.* 39–40 (1998) 759–764.
- [9] K. Walton, The effective elastic modulus of a random packing of sphere, *J. Mech. Phys. Solids* 35 (2) (1987) 213–226.